JOURNAL OF COMPUTATIONAL PHYSICS 9, 568–583 (1972)

Self-Adjusting Hybrid Schemes for Shock Computations

A. HARTEN AND G. ZWAS

Department of Mathematical Sciences, Tel-Aviv University, Ramat-Aviv, Israel

Received June 15, 1971

A general approach for constructing "hybrid schemes" in order to solve quasilinear hyperbolic initial-value problems is presented. The hybrid schemes are constructed from a first-order accuracy operator which dominates in shock regions and a higher-order operator which produces more accurate results in smooth regions.

The usefulness and accuracy of the method is demonstrated in one- and two-dimensional examples, while overcoming nonlinear instabilities and post-shock oscillations.

INTRODUCTION

In order to overcome the post-shock oscillations that occur when using second- and higher-order accurate schemes, various kinds of artificial viscosity terms were used (see, for example, [10] and [5]). In several spatial dimensions these oscillations can even cause nonlinear instabilities, and in order to be able to calculate shocked flows, multidimensional artificial viscosity terms are needed. Burstein [2] used two one-dimensional terms of this kind, but although his results were satisfactory, the pseudoviscosity terms are relatively complicated, time consuming and are difficult to generalize. Intuitively, it seems clear that for second- and higher-order schemes, higher derivatives are used even near shock-like discontinuities, and that is the reason for overshooting, oscillations and even nonlinear instabilities. For linear hyperbolic equations with discontinuous initial conditions, Godunov [3] and Vreugdenhill [11] showed that nonmonotonic shock profiles *must* occur when second-order schemes are used. For the Lax–Wendroff method in the nonlinear case, an explanation for the oscillations was given, at least for stationary shocks [5, p. 229].

The use of first-order accurate schemes produced smooth shock profiles, as with the Lax staggered method [4], where the shocks were very smeared; even better results were obtained with the Abarbanel–Zwas iterative method [1] or with the use of Shuman filters [9]. Knowing all that, we wanted to construct a second-order scheme, which changes automatically and smoothly to a first-order scheme only in narrow shock regions. We would like to have such self-adjusting schemes,

which could be easily generalized to more dimensions without being too complicated and time consuming.

This will be done in the next chapters for nonlinear hyperbolic systems of conservation form, such as

$$W_t = [F(W)]_x + [G(W)]_y , \tag{1}$$

where

$$F_x = A(W) \cdot W_x ,$$
$$G_y = B(W) \cdot W_y ,$$

and where A and B are matrices which can be simultaneously symmetrized by a similarity transformation, a fact that guarantees hyperbolicity.

All the numerical results reported herein were calculated with a CDC-6600 computer at the Tel-Aviv University computation center.

A One-Dimensional Hybrid Scheme

We propose to construct hybrid schemes made of certain convex combinations of other two schemes, namely, we write

$$W_i^{n+1} = [\theta L_1 + (1 - \theta) L_2] \cdot W_i^n, \tag{2}$$

where $W_i^n = W(t_n , i \Delta x)$, L_1 is a first-order finite difference scheme and L_2 a second(or higher)-order scheme. The dimensionless quantity θ, which will be called the "automatic switch," should be normalized so as to be nonnegative and not more than one. It should have the property

$$\theta = \begin{cases} O(1) & \text{in shock regions} \\ O(h^r) & \text{in smooth regions} \end{cases} \tag{3}$$

where $h = \Delta x$ and r is a large enough integer, so that the high accuracy in smooth regions will be preserved.

An example for (2) can be constructed by taking as L_1 the staggered Lax scheme [4],

$$W_i^{n+1} = L_1 W_i^n = (W_{i+1}^n + W_{i-1}^n)/2 + (\lambda/2)(F_{i+1}^n - F_{i-1}^n) \tag{4}$$

and as L_2 the Lax–Wendroff method [5],

$$W_i^{n+1} = W_i^n + (\lambda/2)(F_{i+1}^n - F_{i-1}^n) + (\lambda^2/2)[A_{i+1/2}^n (F_{i+1}^n - F_i^n) - A_{i-1/2}^n (F_i^n - F_{i-1}^n)]. \tag{5}$$

Here $\lambda = \Delta t/\Delta x = \Delta t/h$ and $A^n_{i+1/2} = A((W^n_{i+1} + W_i{}^n)/2)$. Besides substituting (4) and (5) into (2), we want the switch θ to be represented so as to fit into the conservation form of L_1 and L_2. This is important since $\theta = \theta_i{}^n$, and since it is well known that only proper conservation forms produce correct shock velocities (see [8], for example). These considerations lead to the scheme

$$\begin{aligned} W_i^{n+1} = W_i{}^n &+ (\lambda/2)(F^n_{i+1} - F^n_{i-1}) + (\lambda^2/2)[(1 - \theta^n_{i+1/2})\, A^n_{i+1/2}(F^n_{i+1} - F_i{}^n) \\ &- (1 - \theta^n_{i-1/2})\, A^n_{i-1/2}(F_i{}^n - F^n_{i-1})] \\ &+ \tfrac{1}{2}[\theta^n_{i+1/2}(W^n_{i+1} - W_i{}^n) - \theta^n_{i-1/2}(W_i{}^n - W^n_{i-1})]. \end{aligned} \tag{6}$$

This scheme adds to the Lax–Wendroff operator the dissipative terms

$$\begin{aligned} &\tfrac{1}{2}\theta^n_{i+1/2}[(W^n_{i+1} - W_i{}^n) - \lambda^2 A^n_{i+1/2}(F^n_{i+1} - F_i{}^n)] \\ &\quad - \tfrac{1}{2}\theta^n_{i-1/2}[(W_i{}^n - W^n_{i-1}) - \lambda^2 A^n_{i-1/2}(F_i{}^n - F^n_{i-1})]. \end{aligned} \tag{7}$$

We see that θ appears in terms that approximate $\frac{1}{2}h^2(\theta W_x)_x$ and $\frac{1}{2}(\Delta t)^2(\theta A F_x)_x$, and if $\theta = O(h)$ in smooth regions then the second-order accuracy is preserved there. If L_2 is taken to be of l-th-order accuracy then we need $\theta = O(h^m)$, where $m \geqslant l - 1$. In shock regions, property (3) implies the domination of L_1 as long as the switch θ senses strong shock-like gradients; in this sense, the scheme is self-adjusting. The structure of θ will be dealt with later.

Local Monotonicity Requirements

We bring now a linear monotonicity analysis in order to find out which additional conditions should be imposed on θ, such that monotonic behavior near shocks can be expected. We shall use two different methods due to Lax and Wendroff [5], and Godunov [3]; both methods yield the same condition.

Lax and Wendroff [5, p. 228] took a stationary shock and obtained for their scheme, without artificial viscosity terms, the equation

$$(A + \lambda A^2)_{i+1/2} \cdot (W_{i+1} - W_i) + (A - \lambda A^2)_{i-1/2}(W_i - W_{i-1}) = 0, \tag{8}$$

where the upper index n was omitted. Subsequently they substituted for W a solution of the form

$$W_k = W_0 + r^{k+1} W_1 \tag{9}$$

and applied the spectral mapping theorem to get

$$r = (\lambda\mu - 1)/(\lambda\mu + 1), \tag{10}$$

where μ is any one of the eigenvalues of A. Since for stability $\lambda \mid \mu \mid < 1$ is needed, Lax–Wendroff's r is nowhere positive and explains the post-shock oscillation [5, p. 229–230]. Doing the same with our hybrid scheme (6) we obtain

$$\{\theta I + \lambda A + (1 - \theta)\lambda^2 A^2\}_{i+1/2}(W_{i+1} - W_i) + \{-\theta I + \lambda A - (1 - \theta)\lambda^2 A^2\}_{i-1/2}(W_i - W_{i-1}) = 0. \tag{11}$$

Substituting (9) into (11) and applying the spectral-mapping theorem leads to

$$r = [\theta(1 - \lambda^2\mu^2) - \lambda\mu(1 - \lambda\mu)]/[\theta(1 - \lambda^2\mu^2) + \lambda\mu(1 + \lambda\mu)] \qquad (\lambda \mid \mu \mid \leqslant 1). \tag{12}$$

The case $\theta = 1$ yields the positive r corresponding to the first-order Lax scheme [4]. Imposing $r \geqslant 0$, and knowing that θ does not exceed one, we obtain that the condition

$$\lambda \mid \mu \mid /(1 + \lambda \mid \mu \mid) \leqslant \theta \leqslant 1, \tag{13}$$

must be met in shock regions.

Godunov [3] uses a different approach and imposes monotonicity on schemes for solving $U_t = CU_x$ due to the fact that if U is monotonic at $t = 0$, the exact solution will remain monotonic for every $t \geqslant 0$. For the constant-coefficient case it is enough to test a step function (see [3]).

Let us now take θ to be locally constant, and substitute the step function

$$U_i^0 = \begin{cases} 0 & i \leqslant 0 \\ 1 & i > 0 \end{cases} \tag{14}$$

into our hybrid scheme (6) for the equation $U_t = CU_x$ $(C > 0)$. The difference solution after a single time step turns out to be

$$\begin{aligned} U_i^1 &= 0, && (i < 0), \\ U_0^1 &= (z/2)(1 + z) + (\theta/2)(1 - z^2), && (i = 0), \\ U_1^1 &= 1 + (z/2)(1 - z) - (\theta/2)(1 - z^2), && (i = 1), \\ U_i^1 &= 1, && (i > 1), \end{aligned} \tag{15}$$

where $z = \lambda C$ and $z \leqslant 1$ to ensure stability. Imposing monotonicity on (15) yields $\theta(1 - z^2) \geqslant z(1 - z)$ which leads exactly to (13).

STABILITY ANALYSIS

In the linear stability analysis, A is taken to be locally constant as usual, but here we assume that θ can be taken as locally constant too. This seems to be justified in view of the fact that $0 \leqslant \theta \leqslant 1$, and its values certainly do not vary more drastically then the "locally constant" $A(W)$. The numerical results, presented in the final two sections, support that assumption *a posteriori*. As the matrices A and B are symmetrizable by the same similarity transformation, it is enough to investigate the case where A and B are already symmetric. In this case if L_1 and L_2 obey the Von Neumann condition, then $\| L_1 \| \leqslant 1$, $\| L_2 \| \leqslant 1$, and

$$\| L \| = \| \theta L_1 + (1 - \theta) L_2 \| \leqslant \theta \| L_1 \| + (1 - \theta) \| L_2 \| \leqslant 1, \tag{16}$$

where L is the hybrid scheme in question and $\| \cdot \|$ is the appropriate norm. If we now take the stability requirements for L_1 and L_2 separately, we see that the stricter criteria of the two, implies the stability of L. This is the rule for any number of spatial dimensions and every suitable basic scheme L_1 and L_2. In the one-dimensional case for the hybrid scheme (6) the stability condition is

$$\lambda = \Delta t_n / \Delta x \leqslant 1 / | \sigma_j^n |, \tag{17}$$

where σ_j^n is the largest eigenvalue (in absolute value) of A. The numerical radius can replace the norm in (16) as shown in (30).

In order to gain more insight into the stability properties of (6) we perform the usual Fourier transformation and denote by $\xi = k \cdot \Delta x$ the dual variable. The amplification matrix of (6) is

$$G = I + i\lambda A \sin \xi + (\cos \xi - 1)[\theta I + (1 - \theta) \lambda^2 A^2] \tag{18}$$

and by using the spectral-mapping theorem we have

$$| g |^2 = \{1 - (1 - \cos \xi)[\theta + (1 - \theta) \lambda^2 A^2]\}^2 + \lambda^2 a^2 \sin^2 \xi, \tag{19}$$

where g and a are the corresponding eigenvalues of G and A. After rearrangement of terms, (19) takes the form

$$| g |^2 = 1 - 4z(1 - \lambda^2 a^2)[\lambda^2 a^2 (1 - \theta)^2 z + \theta(1 - \theta z)], \tag{20}$$

where $z = \sin^2(\xi/2)$. Note that when $a = 0$ and $0 < \theta < 1$ we have $| g |^2 < 1$ for all $0 < | \xi | \leqslant \pi$; this is of importance for cases in which some of the eigenvalues of A vanish [2, p. 209–210].

THE AUTOMATIC SWITCH

Up to now we have imposed on the switch θ the following properties:

(I) Sensitivity to shock-like discontinuities [$\theta = O(1)$ in shock regions],

(II) Monotonicity in shock regions ($1/2 \leqslant \theta_{\max} \leqslant 1$), (see (13)),

(III) Convexity of the combination of the two basic schemes ($0 \leqslant \theta \leqslant 1$),

(IV) Absence of effect on the l-th-order accuracy in smooth regions [$\theta = O(h^m)$, $m \geqslant l - 1$],

(V) Representation in conservation form [as in (6)].

We see that θ must attain its maximum $\theta_{\max}$ at the shock (at the largest shock if there are a few) and $1/2 \leqslant \theta_{\max} \leqslant 1$. It is also desired that θ will decrease sharply to $O(h^{l-1})$ on both sides of shocks.

Let us now consider any function μ of the dependent variable which is a good sensor of shocks. We select for the sake of simplicity the largest eigenvalue of A as such a function μ.

A possible choice for θ is a *normalized* pseudoviscosity term

$$\theta_{i+1/2} = \chi \left(\frac{| \mu_{i+1} - \mu_i |}{\max_k | \mu_{k+1} - \mu_k |} \right)^m, \tag{21}$$

where $m \geqslant l - 1$ and $1/2 \leqslant \chi \leqslant 1$. A switch like (21) can be substituted into (6) which is in conservation form; it is a dimensionless quantity which serves as a mathematical device without having any physical, or pseudophysical meaning.

At the sharpest gradient within the shock region, $| \mu_{i+1} - \mu_i | = O(1)$ and $\theta = \chi$. In smooth regions, $\theta = O(h^m) \leqslant O(h^{l-1})$, since then $| \mu_{i-1} - \mu_i | = O(h)$. Whenever the solution contains shocks, the denominator in (21) is $O(1)$, a fact that is uneffected by mesh refinements. This is so since for suitable basic schemes, like that of Lax–Wendroff, the number of cells in a shock is independent of h, namely, refinements imply sharper shocks. The fact that θ is normalized is very beneficial in our analysis but can be dangerous in the following situations:

(i) When the solution is (or still is) continuous and the l-th-order accuracy is desired everywhere.

(ii) When the solution contains, in addition to shocks, strong rarefactions so that there is a possibility of getting the maximal θ at a rarefaction. This will not occur for a fine enough grid since mesh refinements do sharpen shocks but do not change rarefaction gradients.

A remedy for these situations can be to insert a check which allows the use of a

nonzero θ *only* when strong enough shock-like gradients are present. In addition, a much sharper θ can be used as, for example,

$$\theta_{i+1/2} = \chi \cdot \exp\left\{1 - \left(\frac{\max_k |\mu_{k+1} - \mu_k|}{|\mu_{i+1} - \mu_i|}\right)^m\right\}. \tag{22}$$

In dealing with hydrodynamic problems we can also use a method proposed by Rosenbluth [7, p. 313], namely, allow $\theta \neq 0$ only where compression occurs. Doing this, expression (21) takes the form

$$\theta_{i+1/2} = \begin{cases} \chi\left(\dfrac{|\mu_{i+1} - \mu_i|}{\max|\mu_{k+1} - \mu_k|}\right)^m, & (\pm)(\mu_{i+1} - \mu_i) < 0, \quad \text{compression} \\ 0, & (\pm)(\mu_{i+1} - \mu_i) \geqslant 0, \quad \text{rarefaction.} \end{cases} \tag{23}$$

The maximum, here, is taken over compression regions only.

The quantity $(\mu_{i+1} - \mu_i)$ changes sign when crossing from rarefaction (diverging characteristics) to compression (converging characteristics); the appropriate sign depends on the choice of μ and the direction of the spatial variable. A similar form can be given to (22). A larger χ, within the range $1/2 \leqslant \chi \leqslant 1$, will yield smoother results but wider shocks. This can be expected and the optimal χ must be chosen so as to achieve a compromise between the smoothness and sharpness of the shock profiles. While the choice $\chi = 1$ means that at a single point only L_1 is used; $\chi = 1/2$ gives equal weight to L_1 and L_2 at the strongest shock-gradient point.

The self-adjusting hybrid schemes deal very well with cases containing several shocks. For example, problems of shallow flows over a ridge were very successfully solved with the proposed methods.[1] In such cases it is best to take the minimal allowed m, namely, $m = l - 1$, in order to prevent giving insufficient weight to L_1 near the weaker shocks.

Two-Dimensional Hybrid Schemes

When dealing with two-dimensional conservation laws like (1) we can take as L_1 an extended staggered Lax scheme,

$$W^{n+1}_{i,j} = (W^n_{i,j+1} + W^n_{i,j-1} + W^n_{i+1,j} + W^n_{i-1,j})/4 + (\lambda/2)(F^n_{i+1,j} - F^n_{i-1,j}) + (\lambda/2)(G^n_{i,j+1} - G^n_{i,j-1}), \tag{24}$$

[1] These results were obtained by U. Asher of Tel-Aviv University who used (23) with $m = 1$ substituted into (6).

where the stability requirement turns out to be

$$\lambda = (\Delta t/h) \leqslant (1/2\sigma). \tag{25}$$

Here $h = \Delta x = \Delta y$, and σ is the spectral radius of $A = \text{grad } F$ and $B = \text{grad } G$.

Condition (25) can be easily obtained with the use of the Lax–Wendroff-stability theorem which uses the numerical range of the amplification matrix [6] or [7, p. 88].

As L_2, the two-dimensional Lax–Wendroff scheme can be used with the stability criteria $\lambda\sigma < 1/\sqrt{8}$. The improved Lax–Wendroff scheme, with a stabilizing fourth-order term and the stability criteria (25), is even better, since then (25) can be used for the hybrid scheme. Two-step second-order schemes as well as third- or fourth-order methods can play the role of the higher-order basic scheme. A hybrid scheme using (24) together with the Lax–Wendroff method is given by

$$\begin{aligned}
W_{i,j}^{n+1} = {} & W_{i,j}^{n} + (\lambda/2)(F_{i+1,j}^{n} - F_{i-1,j}^{n}) + (\lambda/2)(G_{i,j+1}^{n} - G_{i,j-1}^{n}) \\
& + (\lambda^2/2)\{(1 - \theta_{i+1/2,j}^{x})\, A_{i+1/2,j}^{n}[(F_{i+1,j}^{n} - F_{i,j}^{n}) \\
& + \tfrac{1}{4}(G_{i+1,j+1}^{n} + G_{i,j+1}^{n} - G_{i+1,j-1}^{n} - G_{i,j-1}^{n})] \\
& - (1 - \theta_{i-1/2,j}^{x})\, A_{i-1/2,j}^{n}[(F_{i,j}^{n} - F_{i-1,j}^{n}) \\
& + \tfrac{1}{4}(G_{i,j+1}^{n} + G_{i-1,j+1}^{n} - G_{i,j-1}^{n} - G_{i-1,j-1}^{n})]\} \\
& + (\lambda^2/2)\{(1 - \theta_{i,j+1/2}^{y})\, B_{i,j+1/2}^{n}[(G_{i,j+1}^{n} - G_{i,j}^{n}) \\
& + \tfrac{1}{4}(F_{i+1,j+1}^{n} + F_{i+1,j}^{n} - F_{i-1,j+1}^{n} - F_{i-1,j}^{n})] \\
& - (1 - \theta_{i,j-1/2}^{y})\, B_{i,j-1/2}^{n}[(G_{i,j}^{n} - G_{i,j-1}^{n}) \\
& + \tfrac{1}{4}(F_{i+1,j}^{n} + F_{i+1,j-1}^{n} - F_{i-1,j}^{n} - F_{i-1,j-1}^{n})]\} \\
& + \tfrac{1}{4}[\theta_{i+1/2,j}^{x}(W_{i+1,j}^{n} - W_{i,j}^{n}) - \theta_{i-1/2,j}^{x}(W_{i,j}^{n} - W_{i-1,j}^{n})] \\
& + \tfrac{1}{4}[\theta_{i,j+1/2}^{y}(W_{i,j+1}^{n} - W_{i,j}^{n}) - \theta_{i,j-1/2}^{y}(W_{i,j}^{n} - W_{i,j-1}^{n})].
\end{aligned} \tag{26}$$

Note that (26) is represented in conservation form since the right-hand side approximates

$$\begin{aligned}
& W + \Delta t(F_x + G_y) + [(\Delta t)^2/2]\{[(1 - \theta^x)\, A(F_x + G_y)]_x + [(1 - \theta^y)\, B(F_x + G_y)]_y\} \\
& \quad + \tfrac{1}{4}(\Delta x)^2(\theta^x W_x)_x + \tfrac{1}{4}(\Delta y)^2(\theta^y W_y)_y\,.
\end{aligned}$$

It should be remembered that the θ's here are at least $O(h)$ in smooth regions. A fourth-order stabilizing term, approximating $(-\lambda^2/8)\, h^4(1 - \theta)(A^2 + B^2)\, W_{xxyy}$, should be added to (26) in order to use (25) as the final stability condition, otherwise the stability requirement is $\lambda\sigma \leqslant 1/\sqrt{8}$ (see [6]).

The switches θ^x, θ^y can be taken as

$$\theta^x_{i+1/2,j} = \chi\left(\frac{|\mu_{i+1,j} - \mu_{i,j}|}{\max_{s,k}|\mu_{s+1,k} - \mu_{s,k}|}\right)^m, \qquad 1/2 \leqslant \chi \leqslant 1, \quad m \geqslant l-1,$$
$$\theta^y_{i,j+1/2} = \chi\left(\frac{|\mu_{i,j+1} - \mu_{i,j}|}{\max_{s,k}|\mu_{s,k+1} - \mu_{s,k}|}\right)^m. \tag{27}$$

Similarly two-dimensional versions of (22) and (23) can be easily written down. The extension to three dimensions is obvious.

As already mentioned, the stricter stability criteria between those of L_1 and L_2 is the final condition for $L = \theta L_1 + (1-\theta) L_2$. Now L_1, given by (24), has the amplification matrix

$$G_1 = \left(1 - \sin^2\frac{\xi}{2} - \sin^2\frac{\eta}{2}\right) I + i\lambda(A \sin\xi + B \sin\eta) \tag{28}$$

and we will denote by G_2 and G_2' the amplification matrices corresponding to the Lax–Wendroff and the modified L–W schemes, respectively.

If q is any unit vector, then it is shown in [6] that

$$|(G_2 q, q)|^2 \leqslant 1 - |\tilde{A}q|^2(1 - 8|\tilde{A}q|^2)(1-\cos\xi)^2 - |\tilde{B}q|^2(1 - 8|\tilde{B}q|^2)(1-\cos\eta)^2, \tag{29a}$$

$$|(G_2' q, q)|^2 \leqslant 1 - [2 - \cos\xi - \cos\eta]\cdot[(1-\cos\xi)|\tilde{A}q|^2 + (1-\cos\eta)|\tilde{B}q|^2]\cdot[1 - 2|\tilde{A}q|^2 - 2|\tilde{B}q|^2], \tag{29b}$$

and similarly we get

$$|(G_1 q, q)|^2 \leqslant 1 - \tfrac{1}{2}\sin^2\xi(1 - 4|\tilde{A}q|^2) - \tfrac{1}{2}\sin^2\eta(1 - 4|\tilde{B}q|^2), \tag{29c}$$

where $\tilde{A} = \lambda A$, $\tilde{B} = \lambda B$, and where ξ and η are the dual variables after the usual Fourier transform.

In the linearized version, $G = \theta G_1 + (1-\theta) G_2'$. Using (29) and imposing (25) (or $\lambda\sigma < 1/\sqrt{8}$ if G_2 replaces G_2') we find that linear stability is achieved, since

$$|(Gq, q)| \leqslant \theta|(G_1 q, q)| + (1-\theta)|(G_2' q, q)| \leqslant 1. \tag{30}$$

Examining now the case where $|Aq| = |Bq| = 0$ we see that $|(G_2 q, q)| = |(G_2' q, q)| = 1$; this situation is possible if and only if zero is an eigenvalue of A and B. For this case the numerical range, as computed from (28) is $|(G_1 q, q)| = 1 - \sin^2(\xi/2) - \sin^2(\eta/2)$ and we see that for $0 < \theta \leqslant 1$, $|(Gq, q)| < 1$ for all $0 < |\xi|; |\eta| \leqslant \pi$. Consequently, our scheme has a damping effect, including the case when zero is an eigenvalue of A and B (stagnation points, etc.

[2, p. 209–210]); this is not so for $\theta \equiv 0$, namely, for the pure Lax–Wendroff scheme.

Numerical Results in One Dimension

Among the one-dimensional problems that were actually solved we will bring the results of two sets of examples: (I) a mathematical-model equation with a known solution used for checking the accuracy achieved in smooth regions, and the shock profiles produced; (II) a one-dimensional hydrodynamic shock for solving a physical problem and checking the numerical shock speed.

First we take the equation

$$u_t + uu_x = 0 \tag{31}$$

with the initial conditions

$$u(0, x) = \begin{cases} 1 & x \leqslant 0, \\ 1 - x & 0 \leqslant x \leqslant 1, \\ x - 1 & 1 \leqslant x \leqslant 2, \\ 1 & 2 \leqslant x. \end{cases} \tag{32}$$

In this case there is a compression region which gradually leads to a shock at the time $t = 1$, and a rarefaction wave with positive gradients which decrease in time. The exact solution is[2]

$$u(x, t) = \begin{cases} 1 & x \leqslant t, \\ (1 - x)/(1 - t) & t \leqslant x \leqslant 1, \\ (x - 1)/(t + 1) & 1 \leqslant x \leqslant 2 + t \\ 1 & 2 + t \leqslant x, \end{cases} \quad \begin{pmatrix} 0 \leqslant t < 1, \\ \text{continuous} \end{pmatrix}, \tag{33a}$$

and

$$u(x, t) = \begin{cases} 1, & x < 2 + t - \tau \\ (x - 1)/(t + 1), & 2 + t - \tau \leqslant x \leqslant 2 + t \\ 1, & 2 + t \leqslant x \end{cases} \quad \begin{pmatrix} 1 \leqslant t, \\ \tau = (2 + 2t)^{1/2}, \\ \text{discontinuous} \end{pmatrix} \tag{33b}$$

The results after 300 time steps are shown in Figs. 1 and 2, where the exact solution is plotted for each graph together with the numerical solution. In all the cases, $h = 0.05$ and $0 \leqslant x \leqslant 20$ were taken. Graph (1a) shows the solution obtained with the first-order staggered method given by (4), graph (1b) was

[2] This problem was suggested to us by M. Goldberg who used it in his Ph.D. thesis, Tel-Aviv University. He too, applied first order methods in shocks only, using his own technique.

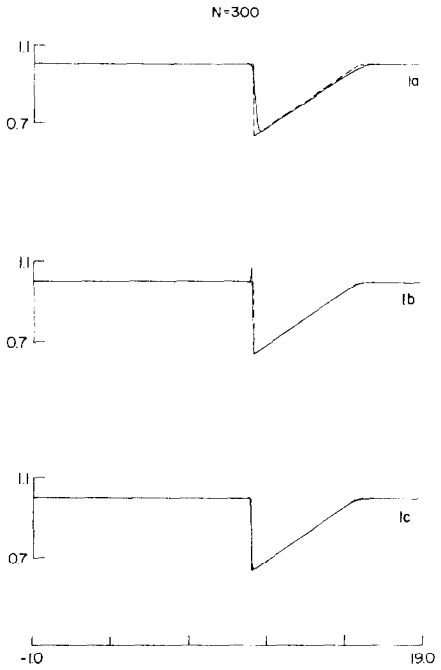

FIGURE 1

produced by the Lax–Wendroff scheme, graph (1c) was obtained with a hybrid scheme using the switch (22) with $\chi = 1/2$, $m = 2$ and where χ is taken to be zero at rarefaction regions.

Figure 2 shows the results of the same problem with switch (23), $m = 1$, and $\chi = 1., 0.5, 0.3$ for (2a), (2b), (2c) respectively. Graph (2c) demonstrates that when $\theta_{\max} = \chi$ is less than $1/2$ the monotonicity is violated. Notice the correctness of the shock speed and the high accuracy at the smooth regions. This high accuracy is such that the numerical values corresponding to graphs (1b) and (2b), are the same up to 6 significant decimal places everywhere except in the narrow shock region. The width of the shock region in graph (2b) is almost as small as in graph (1b) and is much smaller than in graph (1a).

As a second one-dimensional example, we take the hydrodynamic system of equations in Lagrangean formulation [7, Chapter 12],

$$\begin{bmatrix} V \\ u \\ E \end{bmatrix}_t + \begin{bmatrix} -u \\ P \\ Pu \end{bmatrix}_x = 0 \qquad (V_0 = 1). \tag{34}$$

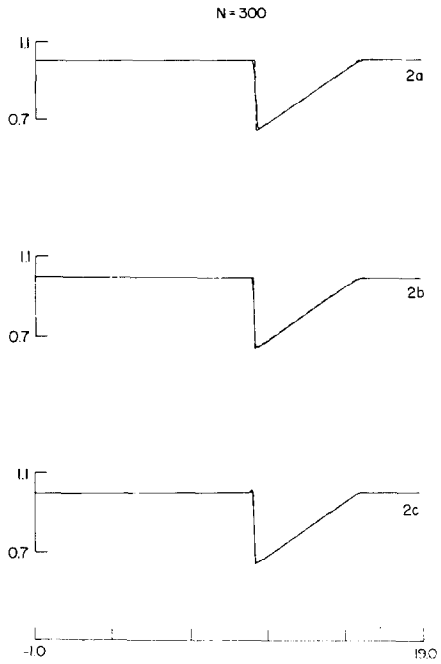

FIGURE 2

Here V, u, E and P are the specific volume, the velocity, the total energy per unit mass and the pressure, respectively. We take the simple equation of state $P = (\gamma - 1)(E - 1/2u^2)/V$, where γ is the polytropic constant. The eigenvalues of $A = \text{grad}\, F$ [$F = (u, -P, -Pu)$], are 0, $\pm C$, where C is the Lagrangean sound speed given by $(\gamma P/V)^{1/2}$. We solved some problems of stationary shocks with different values of γ and different shock strengths (namely, different pressure ratios at the shock), corresponding to all the cases solved in [1].

Figure 3 shows the pressure for $\gamma = 1.4$, pressure ratio of 10, after 200 time steps. Graph (3b) was produced by the Lax–Wendroff method and graph (3c) with the hybrid method (6) using the switch (23) with $\mu = C$, $m = 1$, $\chi = 0.5$. Graph (3a) shows for comparison the shock obtained with the staggered Lax method.

All the conclusions arrived at for the simple Equation (31) were found to be valid for the system (34). The shock speed for graph (3c) is as correct as for (3a); the shock width is by 1–2 cells larger than in [2] but much smaller than the corresponding width of first-order methods.

Of course the Lax–Wendroff scheme could be used with nonlinear artificial viscosity (see [5]) but this is much more time consuming (especially in more dimensions), and much harder to generalize to several dimensions, as we shall see later.

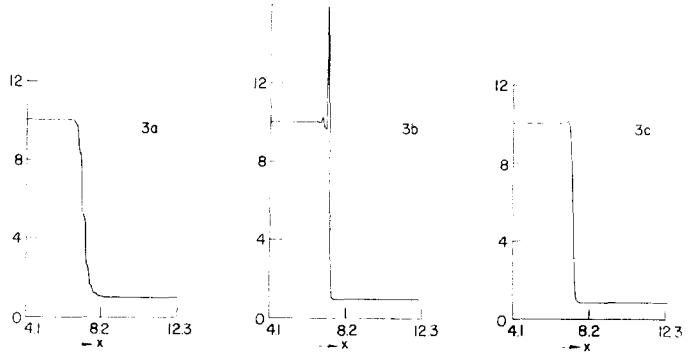

FIGURE 3

TWO-DIMENSIONAL RESULTS

We choose the example of calculating a detached shock in front of a rectangular body moving with constant supersonic speed along its axis of symmetry. This problem was solved by Burstein [2], who used the Lax–Wendroff two-dimensional scheme with two one-dimensional artificial viscosity terms.

In order to submit our scheme to a hard test we chose impulsive initial conditions, i.e., the body appeared impulsively at $t = 0$ in the supersonic flow. We solved this problem with a hybrid scheme as well as with Burstein's method, where the Eulerian formulation was taken, i.e., the equations are

$$\begin{bmatrix} \rho \\ m \\ n \\ E \end{bmatrix}_t + \begin{bmatrix} m \\ \dfrac{3-\gamma}{2}\cdot\dfrac{m^2}{\rho} + f_1 \\ \dfrac{mn}{\rho} \\ f_2 + \dfrac{\gamma m E}{\rho} \end{bmatrix}_x + \begin{bmatrix} n \\ \dfrac{mn}{\rho} \\ \dfrac{3-\gamma}{2}\cdot\dfrac{n^2}{\rho} + g_1 \\ g_2 + \dfrac{\gamma n E}{\rho} \end{bmatrix}_y = 0, \tag{35}$$

where

$$f_1 = (\gamma - 1)\left(E - \frac{n^2}{2\rho}\right); \qquad f_2 = \frac{1-\gamma}{2}\frac{m}{\rho^2}(m^2 + n^2),$$

$$g_1 = (\gamma - 1)\left(E - \frac{m^2}{2\rho}\right); \qquad g_2 = \frac{1-\gamma}{2}\frac{n}{\rho^2}(m^2 + n^2).$$

Here ρ, m, n and E are the density, the momentum in the x direction ($m = \rho u$), the momentum in the y direction ($n = \rho v$) and the total energy per unit volume,

respectively. The pressure was taken as $P = (\gamma - 1)[E - (m^2 + n^2)/(2\rho)]$. As pointed out earlier, any function which is a good sensor of shocks is suitable for constructing the switches.

We chose

$$\theta^x_{i+1/2,j} = \chi \left(\frac{| \rho_{i+1,j} - \rho_{i,j} |}{\max | \rho_{l+1,k} - \rho_{l,k} |} \right)^2, \tag{36a}$$

$$\theta^y_{i,j+1/2} = \chi \left(\frac{| \rho_{i,j+1} - \rho_{i,j} |}{\max | \rho_{l,k+1} - \rho_{l,k} |} \right)^2, \tag{36b}$$

where the maximum is taken over compression regions only, i.e., for all l and k such that $\rho_{l+1,k} > \rho_{l,k}$ in (36a) and $\rho_{l,k+1} < \rho_{l,k}$ in (36b). χ will be specified in (38).

In (36) the pressure P can replace the density ρ if desired. The quadratic θ's were chosen to ensure sharp switches in order to produce sharp shocks. The boundaries were treated according to Vliegenthart's suggestions [9], except that we took higher-order extrapolations whose directions fall into the appropriate domain of influence.

We show below some results of stationary density profiles along lines parallel to the axis of symmetry for different values of y. The initial conditions for these cases are

$$\begin{aligned} &\gamma = 1.4; \quad P = 1; \quad \rho = 1; \quad n = 0; \\ &m = 5 \quad \text{(namely, a Mach number of } \sim 4.23), \\ &\text{and an impulsive start at } t = 0. \end{aligned} \tag{37}$$

Graph (4a) shows the results with our method, graph (4b) with Burstein's method. In both runs the geometry and mesh size were exactly as specified in [2].

The artificial viscosity constant in Burstein's method {χ in formula (5.3a) in [2]} was taken as 2, since the value of 1 was insufficient for preventing severe nonlinear instabilities, even when changing the constant from 2 to 1 after several hundreds of cycles. The results shown in Fig. (4a) were obtained with the switches (36) substituted in (26), where

$$\chi = \frac{1}{2} \begin{cases} 1 & \rho_{i+1,j} - \rho_{i,j} > 0 \\ \alpha & \rho_{i+1,j} - \rho_{i,j} \leqslant 0, \end{cases} \quad \text{[in (36a)]} \tag{38a}$$

$$\chi = \frac{1}{2} \begin{cases} 1 & \rho_{i,j+1} - \rho_{i,j} < 0 \\ \alpha & \rho_{i,j+1} - \rho_{i,j} \geqslant 0. \end{cases} \quad \text{[in (36b)].} \tag{38b}$$

We propose to take $\alpha = 0$ in general, but for the present problem it was necessary to take a small positive α because of the strong rarefaction gradients near the corner; we have taken $\alpha = 0.05$. The constant α should be small enough so that the θ near the corner will be much smaller than the maximal θ obtained at the shock. At all other smooth regions, (36) yields $\theta = O(h^2)$ which is even one order higher than needed to ensure second-order accuracy.

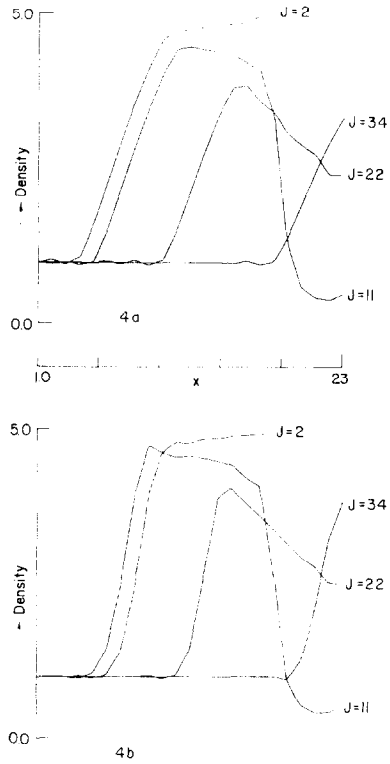

FIGURE 4

It is to be expected that $\alpha = 0$ can be taken for aerodynamical bodies having continuously differentiable surfaces. The need for a small positive α in our problem is necessitated by the corner singularity. The shock in Fig. (4b) has a smoother profile than in Fig. (4a) but occupies 4–5 cells comparted to 3–4 cells in Fig. (4b). Figure 5 shows results of the flow field with the sonic line and the detached shock wave obtained by our method as well as with Burstein's. The results are practically the same except for small differences near the corner; with both these methods the sonic line meets the body at the corner in contrast to first-order results [2, Fig. 6] where the sonic line is smeared along the upper boundary. For both methods approximately 2000 cycles are needed to reach the steady state, when starting with the initial values (28). The flow field is given in Fig. 5 below.

The self-adjusting hybrid scheme has several advantages. Firstly, it saves considerable computing time; it takes less than half the time per cycle compared to Burstein's method. This advantage is even more considerable for three dimensions. Secondly, its structure is general; better schemes than Lax–Wendroff's can be used

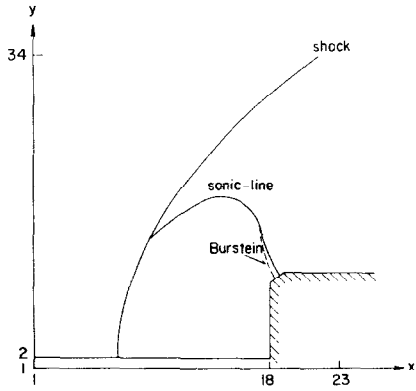

FIGURE 5

for L_2 as, for example, optimally stable schemes, third- or fourth-order schemes, etc.

Additional advantages are the freedom in choosing a suitable numerical switch as well as the easy insertion of the hybridization technique into existing computer programs for solving problems containing discontinuities.

REFERENCES

1. S. ABARBANEL AND G. ZWAS, An iterative finite difference method for hyperbolic systems, *Math. Comp.* **23** (1969), 549–565.
2. S. Z. BURSTEIN, Finite difference calculations for hydrodynamic flows containing discontinuities, *J. Computational Phys.* **2** (1967), 198–222.
3. S. K. GODUNOV, Finite difference methods for numerical computation of discontinuous solutions of the equations of fluid dynamics, *Mat. Sb.* **47** (1959), 271–295.
4. P. D. LAX, Weak solutions of nonlinear hyperbolic equations and their numerical computations, *Comm. Pure Appl. Math.* **7** (1954), 159–193.
5. P. D. LAX AND B. WENDROFF, Systems of conservation laws, *Comm. Pure Appl. Math.* **13** (1960), 217–237.
6. P. D. LAX AND B. WENDROFF, Difference schemes for hyperbolic equations with high order of accuracy, *Comm. Pure Appl. Math.* **17** (1964), 381–398.
7. R. D. RICHTMYER AND K. W. MORTON, "Finite Difference Methods for Initial Value Problems," Interscience, New York, 1967.
8. B. VAN LEER, Stabilization of difference schemes for the equations of inviscid compressible flow, *J. Computational Phys.* **3** (1969), 473–485.
9. A. C. VLIEGENTHART, The Shuman filtering operator and the numerical computation of shock waves, *J. Engrg. Math.* **4** (1970), 341–348.
10. J. VON NEUMANN AND R. D. RICHTMYER, A method for the numerical calculation of hydrodynamic shocks, *J. Appl. Phys.* **21** (1950), 232–237.
11. C. B. VREUGDENHILL, On the effect of artificial viscosity methods in calculating shocks, *J. Engrg. Math.* **3** (1969), 285–288.